Published in final edited form as:
Nat Genet. 2013 January ; 45(1): 93–97. doi:10.1038/ng.2492.

Mutations in *AP2S1* cause familial hypocalciuric hypercalcemia type 3

M. Andrew Nesbit[1], **Fadil M. Hannan**[1], **Sarah A. Howles**[1], **Anita A.C. Reed**[1], **Treena Cranston**[2], **Clare E. Thakker**[1], **Lorna Gregory**[3], **Andrew J. Rimmer**[3], **Nigel Rust**[4], **Una Graham**[5], **Patrick J. Morrison**[6], **Steven J. Hunter**[5], **Michael P. Whyte**[7], **Gil McVean**[3], **David Buck**[3], and **Rajesh V. Thakker**[1]

[1]Academic Endocrine Unit, Nuffield Department of Clinical Medicine, University of Oxford, Oxford, United Kingdom.

[2]Oxford Molecular Genetics Laboratory, Churchill Hospital, Oxford, United Kingdom.

[3]Wellcome Trust Centre for Human Genetics, Roosevelt Drive, University of Oxford, Oxford, United Kingdom.

[4]Sir William Dunn School of Pathology, University of Oxford, Oxford, United Kingdom

[5]Regional Centre for Endocrinology and Diabetes, Royal Victoria Hospital, Belfast, United Kingdom.

[6]Department of Medical Genetics, Queen's University Belfast, Belfast City Hospital, Lisburn Road, Belfast, United Kingdom.

[7]Center for Metabolic Bone Disease and Molecular Research, Shriners Hospital for Children, St. Louis, USA.

Abstract

Adaptor protein-2 (AP2), a central component of clathrin-coated vesicles (CCVs), is pivotal in clathrin-mediated endocytosis which internalises plasma membrane constituents such as G protein-coupled receptors (GPCRs)[1-3] . AP2, a heterotetramer of alpha, beta, mu and sigma subunits, links clathrin to vesicle membranes and binds to tyrosine-based and dileucine-based motifs of membrane-associated cargo proteins[1,4]. Here, we show that AP2 sigma subunit (*AP2S1*) missense mutations, which all involved the Arg15 residue (Arg15Cys, Arg15His and Arg15Leu) that forms key contacts with dileucine-based motifs of CCV cargo proteins[4], result in familial hypocalciuric hypercalcemia type 3 (FHH3), an extracellular-calcium homeostasis disorder

Correspondence and requests for materials should be addressed to R.V.T. (rajesh.thakker@ndm.ox.ac.uk)..

URLs
Stampy: http://www.well.ox.ac.uk/project-stampy; Platypus: (http://www.well.ox.ac.uk/platypus); Polyphen-22: (genetics.bwh.harvard.edu/pph2/); SIFT: (sift.jcvi.org/); MutationTaster: (www.mutationtaster.org/); Exome Variant Server. NHLBI Exome Sequencing Project (ESP). Seattle, WA: (http://evs.gs.washington.edu/EVS/)

Accession codes The AP2S1 references sequence is available at GenBank under accessionNM_004069.3[13].

Author Contributions M.A.N. and R.V.T. designed the experiments. M.A.N., F.M.H., S.A.H., A.A.C.R., C.E.T. performed experiments and analysed data. M.A.N., S.A.H., A.A.C.R., T.C., C.E.T., L.G. and A.R. carried out sequencing and information technology. G.M. and D.B. directed the information technology and the exome capture DNA sequencing infrastructure. T.C., U.G., P.J.M., S.J.H., M.P.W. and R.V.T. recruited FHH subjects and families. M.A.N., F.M.H., S.A.H. and N.R. performed the AP2S1 functional calcium assays. M.A.N., F.M.H. and R.V.T. wrote the manuscript. All authors checked for scientific content and contributed to the final drafting of the manuscript.

Author Information Reprints and permissions information is available at www.nature.com/reprints/index.html. The authors declare that they have no competing financial interests. Readers are welcome to comments on the online version of this article at www.nature.com/nature.

Europe PMC Funders Author Manuscripts

affecting parathyroids, kidneys and bone[5-7] These *AP2S1* mutations occurred in >20% of FHH patients without calcium-sensing GPCR (CaSR) mutations which cause FHH1[8-12]. *AP2S1* mutations decreased the sensitivity of CaSR-expressing cells to extracellular-calcium and reduced CaSR endocytosis, likely through a loss of interaction with a C-terminus CaSR dileucine-based motif whose disruption also decreased intracellular signalling. Thus, our results reveal a new role for AP2 in extracellular-calcium homeostasis.

AP2S1 mutations were initially identified by exome capture and high-throughput sequence analysis of genomic DNA from an affected individual from each of two unrelated kindreds with FHH3 ($FHH3_{OK}$ and $FHH3_{NI}$, Table 1 and Supplementary Fig. 1)[5-7]. This revealed the occurrence of over 2500 previously unreported non-synonymous single nucleotide variants (SNVs) in the whole exome of each patient. An analysis of SNVs within the 3.46Mbp interval on 19q13.3, which is the location of the *FHH3* locus[6,7] and contains ~110 genes, revealed one SNV, a C to T transition in exon 2 of the *AP2S1* gene, which encodes the protein AP2σ2[13], in patients from both kindreds. The C to T transition, which predicted the occurrence of a missense mutation (Arg15Cys) (Supplementary Fig. 1), was confirmed by dideoxynucleotide sequencing (Supplementary Fig. 1) and the resulting alterations in restriction endonuclease (*HhaI* and *BmgBI*) sites (Supplementary Fig. 1) were used to demonstrate its cosegregation in members (32 affected and 23 unaffected) from 4 generations of the two kindreds (Supplementary Fig. 1).

FHH3, together with FHH1 and FHH2 are genetically heterogenous autosomal dominant disorders of extracellular-calcium (Ca_o^{2+}) homeostasis that are characterised by lifelong elevations of serum calcium concentrations with inappropriately low urinary calcium excretion (mean urinary calcium:creatinine clearance ratio <0.01)[5,9,11]. The loci for FHH1, FHH2, and FHH3 are located on chromosomes 3q21.1, 19p, and 19q13.3, respectively[6-8,14]. FHH1 and FHH2 are usually associated with normal circulating parathyroid hormone (PTH) concentrations and mild hypermagnesemia, and are generally asymptomatic disorders[9,11]; although some FHH1 patients may suffer from pancreatitis, chondrocalcinosis, or primary hyperparathyroidism due to excessive PTH secretion by parathyroid tumours, which in neonates may result in life-threatening hypercalcemia, hypotonia, bone demineralization, fractures and respiratory distress, and in adults may be associated with osteoporosis and kidney stones[9,11]. FHH3 is characterised by different clinical features, which include increased serum PTH concentrations, hypophosphatemia, and osteomalacia[5,7]. Approximately 65% of FHH patients have FHH1, due to loss-of-function mutations of the CaSR, a GPCR encoded by a gene on 3q21.1[8-11]. To determine the frequency of *AP2S1* mutations in the remaining ~35% of FHH patients, we undertook DNA sequence analysis of the 5 exons and 8 intron-exon boundaries of *AP2S1* in 50 unrelated patients in whom CaSR mutations had been excluded[9]. This revealed the occurrence of 11 missense heterozygous mutations, consistent with autosomal dominant inheritance of FHH3, that all affected Arg15 and consisted of four Arg15Cys, three Arg15His, and four Arg15Leu mutations (Table 1 and Supplementary Fig. 1). Patients with these *AP2S1* mutations, whose ages ranged from 8 days to 78 years (Table 1), had similar elevations in serum calcium and PTH concentrations and reductions in urine calcium excretion, thereby indicating an absence of a correlation between the mutation and clinical phenotype. However, the occurrence of these 3 different *AP2S1* mutations that altered only the Arg15 residue in 13 unrelated probands and the significant conservation of the Arg15 residue in 5,400 human exomes ($p<10^{-10}$, Fisher exact test) indicates that this residue represents a likely mutational hotspot. Indeed, Arg15 *AP2S1* missense mutations may be the underlying cause of FHH in >20% of patients without CaSR mutations.

The observations of 13 FHH3-associated *AP2S1* mutations that solely involved the Arg15 residue (Table 1), which is evolutionarily conserved in all AP2σ2 subunit orthologues and human AP sigma subunit paralogues (Fig. 1a)[3], indicated that this residue likely plays a critical role in the AP2 complex. Indeed, an analysis of the crystal structure of AP2 revealed that the Arg15 (R15) residue of AP2σ2 and the Arg21 (R21) residue of AP2α1 are involved in forming key contacts with a glutamine (Q) residue at position −4 relative to the first leucine of the dileucine motif of cargo proteins (Fig. 1b)[4]. Replacing the positively charged Arg15 residue with either the polar, but uncharged, Cys15 (C15) residue (Fig 1c) or the non-polar Leu15 (L15) residue (Fig. 1d) is predicted to lead to a reduced affinity for the dileucine motif, and hence compromise adaptor function. However, the effects of the His15 (H15) mutation (Fig. 1e) are more difficult to predict as arginine and histidine are both positively charged residues. We hypothesised that these predicted effects of the FHH3-associated *AP2S1* mutants may decrease the sensitivity of cells expressing the CaSR to extracellular-calcium (Ca_o^{2+}) and reduce CaSR endocytosis, for the following four reasons. First, AP2 is known to play an important role in GPCR endocytosis and recycling, thereby influencing GPCR sensitivity (Fig. 2)[15]; and second, the CaSR has within its cytoplasmic C-terminal domain a variant dileucine motif (Arg-His-Gln-Pro-Leu-Leu (RHQPLL), residues 1009-1014)[9,16]. Third, the CaSR is pivotal in Ca_o^{2+} homeostasis (Fig. 2), and in mediating changes in PTH secretion and renal tubular calcium reabsorption in response to alterations in plasma calcium concentrations[9-12]; and fourth, CaSR loss-of-function mutations found in patients with the similar disorder of FHH1, cause a decrease in the sensitivity of cells expressing the CaSR[8-10,12,17].

To investigate this hypothesis and the functional effects of the FHH3-associated Arg15Cys, Arg15His and Arg15Leu *AP2S1* mutants, we pursued two approaches . First, we assessed the effects of removing the CaSR dileucine motif, by transient transfection of Human Embryonic Kidney (HEK)293 cells with either wild-type CaSR (Leu-Leu1013-4) or mutant CaSR (Ala-Ala1013-4) and measuring the $[Ca^{2+}]_i$ responses of the transfected cells to alterations in $[Ca^{2+}]_o$, using reported methods[9,12]. We chose HEK293 cells as suitable parathyroid and renal thick ascending limb (TAL) cells are not available and because HEK293 cells are an established model system for assessing CaSR mutants[9,12,18-22]. Moreover, HEK293 cells predominantly express the full-length *AP2S1* transcript at levels that are comparable to that found in human parathyroid adenomas and kidney (Supplementary Fig. 2). Expression of the mutant CaSR led to a rightward shift in the concentration-response curves with a significantly higher EC_{50} (i.e. the $[Ca^{2+}]_o$ required to produce a half-maximal increase in $[Ca^{2+}]_i$) value (mutant EC_{50}=3.63mM (95% confidence interval (CI) 3.57-3.68mM)(n=8) versus wild-type EC_{50}=3.41mM (95% CI 3.36-3.46mM) (n=8), p<0.0001) (Supplementary Fig. 3). Thus, these results indicate that the CaSR dileucine motif is functionally significant. Second, we established HEK293 cells that stably expressed CaSR and transiently transfected them with either wild-type or mutant *AP2S1*-pBI-CMV2 expression constructs. We specifically chose to subclone the full-length coding region of *AP2S1* into the bidirectional vector pBI-CMV2, which contains a green fluorescent protein (GFP) reporter gene (Fig. 3a), as it allowed co-expression of AP2σ2 and GFP at equivalent levels (Fig. 3b) without the requirement of tagging the small (17kDa) AP2σ2 protein that may have altered its function[23]. Following transient transfection with either wild-type or mutant *AP2S1*-pBI-CMV2 constructs, the expression of CaSR, AP2σ2 and GFP, which also represented a surrogate marker for transfected AP2σ2, was detected by immunofluorescence and/or Western blot analysis (Fig. 3a and 3b), and the EC_{50} of the $[Ca^{2+}]_i$ responses to $[Ca^{2+}]_o$ measured[9,12,19,24-26]. This revealed that expression of all three mutant AP2σ2s led to a rightward shift in the concentration–response curves (Fig. 3c-e) with significantly higher EC_{50} (Arg15Cys=2.90mM (95% CI 2.85-2.96mM); Arg15His=2.73mM (95% CI 2.66-2.80mM); Arg15Leu=2.86mM (95% CI 2.80-2.93mM); and wild-type AP2σ2 EC_{50} =2.53mM (95% CI 2.47-2.60mM), all p<0.0001, n=12, when compared to wild-type)

(Table 2). The increase in the CaSR EC_{50} induced by the FHH3-associated *AP2S1* mutants indicate a decrease in the sensitivity of cells expressing CaSR to extracellular-calcium, and this is consistent with the effects of the loss-of-function CaSR mutations reported in FHH1[9,12] . Moreover the EC_{50} values of the cells transfected with the Leu15 and His15 *AP2S1* mutants were similar to that of cells transfected with vector alone, whereas the EC_{50} value of cells transfected with the Cys15 *AP2S1* mutant were significantly higher than those with vector alone, thereby indicating a possible dominant-negative effect for this *AP2S1* mutant (Table 2).

To investigate the effect of the *AP2S1* Arg15 mutations on CaSR endocytosis, we evaluated CaSR cell-surface expression by an intact cell ELISA[18] in HEK293 cells that were stably transfected with CaSR, under basal and stimulated conditions using 0.5mM and 5mM Ca_o^{2+}, respectively (Table 3). The basal cell-surface expression of CaSR in cells trasfected with wild-type or mutant *AP2S1*, or vector alone was similar (Table 3). Increasing $[Ca^{2+}]_o$ resulted in decreased cell-surface expression of CaSR in all cells, whether transfected with wild-type or mutant AP2S1, or vector alone, thereby indicating internalisation of ligand-stimulated CaSR by endocytosis[20], mediated by endogenous wild-type AP2σ2 (Table 3). However, following stimulation with increased $[Ca^{2+}]_o$, cells transfected with wild-type *AP2S1* had a significantly further reduction of cell-surface CaSR expression when compared to those transfected with mutant Arg15Cys *AP2S1* or vector alone, whilst those cells transfected with mutant Arg15Cys *AP2S1* had a similar CaSR cell-surface expression to that observed in cells transfected with vector alone(Table 3). These results indicate that the effect of the transfected wild-type *AP2S1* is to raise the total of available wild-type AP2σ2 (i.e. endogenous plus transfected AP2σ2), which will increase CaSR endocytosis; however, this increased CaSR endocytosis is not observed in cells transfected with the *AP2S1* mutant, which instead is associated with decreased CaSR internalisation (Table 3). Thus, our studies demonstrate that AP2σ2 has a role in CaSR endocytosis as well as in the regulation of CaSR signaling via Ca_i^{2+} (Fig. 2), a pathway pivotal for Ca_o^{2+} homeostasis, such that its disruption by *AP2S1* Arg15 mutants results in FHH3.

Our study, which represents the first report of a disease-causing mutation of an AP2 subunit, demonstrates that missense mutations (Arg15Cys, Arg15His, and Arg15Leu) (Supplementary Fig. 1) of AP2σ2, a ubiquitously expressed protein (Supplementary Fig. 2) that forms part of the AP2 heterotetrameric complex[1], surprisingly does not result in a multi-system disorder but instead results in a specific disorder of extracellular-calcium homeostasis involving the parathyroids, kidneys and bone[5-7]. A possible explanation for this could be that mutation of Arg15, which in an analysis of >50 unrelated FHH patients was found to be the only residue involved, likely has a specific effect such as recognition of the CaSR dileucine motif by AP2σ2. This implies that mutations of other *AP2S1* residues may result in different diseases, and the situation may be analogous to that reported for different mutations of lamin A (*LMNA*), which are associated with six different tissue-specific diseases[27]. Thus, our results which have defined that mutations of a specific residue (Arg15) of AP2σ2 cause FHH3, demonstrate a previously unrecognized role for AP2σ2 in extracellular-calcium homeostasis.

ONLINE METHODS

Patients

Informed consent was obtained from individuals, using protocols approved by the local and national ethics committees (MREC/02/2/93). Thirty-two family members (17 affected members and 15 unaffected members), from four generations, of the previously reported FHH_{OK} kindred[5,6] and 23 family members (16 affected members and 7 unaffected members), from three generations, of the reported FHH_{NI} kindred[7] were investigated. In

addition, 50 reported FHH patients[9] (23 males and 27 females) in whom *CASR* mutations had not been detected, were investigated. Clinical details of the two FHH3 kindreds[5-7] and the FHH patients without CaSR mutations have been reported[9].

Exome capture and DNA sequencing

Leukocyte DNA was prepared from venous blood[6,9], and quantified using the High Sensitivity Qubit system (Invitrogen) and assessed for integrity using an agarose gel. Three μg of DNA were fragmented, and libraries prepared using the SureSelect Human All Exon v2 Kit (Agilent Technologies, Santa Clara, CA), as follows[31]. Fragmented DNA was amplified using universal adapter sequences and the amplified library hybridized to the SureSelect oligos before additional rounds of amplification. Libraries were quality checked using the 2100 Bioanalyzer (Agilent Technologies, Santa Clara, CA), and quantified by qRT-PCR, prior to analysis by an Illumina GAIIx, using 50bp paired end reads[31,32].

Bioinformatic analysis of exome sequence data

Data were aligned to the Human37 reference genome build, using an in-house short-read mapper, (Stampy)[33] and stored in BAM format[34]. Sufficient target region coverage (i.e. >10 base reads) was verified in excess of 70% for the analyzed samples. Identification of variant sites and alleles was performed with an in-house variant-caller, Platypus, which can detect single nucleotide variants (SNVs) and short (<50bp) indels. Variants were reported in a final output VCF file and filtered to reduce the false-positive rate. Variants previously reported in dbSNP v.135 or 1000 Genomes databases were excluded from further analysis. Remaining variants were examined using the programs Polyphen-22, SIFT and MutationTaster to predict the effect on encoded protein, conservation and expression. Aligned reads were viewed with the Integrative Genomics Viewer[35].

Sanger (dideoxynucleotide chain termination) sequencing of *AP2S1*

Leukocyte DNA was used with *AP2S1*-specific primers (Supplementary Table 1)(for PCR amplification of the 5 exons and 8 intron-exon boundaries and the DNA sequences of the PCR products determined using BigDye Terminator v3.1 Cycle Sequencing Kit (Life Technologies, Grand Island, NY) and an ABI 3730 Automated capillary sequencer (Applied Biosystems, Foster City, CA)[9]. DNA sequence abnormalities and co-segregation in families were confirmed by restriction endonuclease analysis (New England Biolabs), as described[24]. In addition, the DNA sequence abnormalities were confirmed by high-resolution melting (HRM) curve analysis using a Rotor-Gene Q (Qiagen Inc, Valencia, CA)[36]. Sequence changes were compared with data from the NHLBI-ESP, which provides the exome sequences from ~5400 samples, to assess whether they represent rare polymorphisms that may occur in 0.1% of the population.

Protein sequence analysis and computer modeling of AP2 structure

Protein sequences of AP2σ2 orthologues and paralogues were aligned with Clustal W[37]. The crystal structure of AP2 heterotetramer bound to an acidic dileucine peptide has been reported[4]. The PyMOL Molecular Graphics System (Version 1.2r3pre, Schrödinger, LLC) was used to model the effect of the FHH3-associated *AP2S1* mutations on the interaction with acidic dileucine motif peptide using three-dimensional structure of AP2 archived in the Protein Data Bank at the European Bioinformatics Institute with the accession number 2JKR[4,25].

Functional expression of *CASR* and *AP2S1* mutations

Functional studies to assess CaSR signalling were performed in HEK293 cells because suitable parathyroid and renal tubular cells are not available, and HEK293 cells have been

established as a model for such studies[9,12,18,19,21,22]. The previously reported CaSR-EGFP construct[9,19] was used and an expression construct for AP2σ2 was generated by cloning the *AP2S1* full-length coding region into the bi-directional cloning vector pBI-CMV2 (Clontech) which allows co-expression of AP2σ2 and GFP at equivalent levels[23]. *CASR* and *AP2S1* mutations were introduced into the construct by site-directed mutagenesis (QuikChange; Stratagene, La Jolla, CA, USA) and confirmed by DNA sequence analysis, as described[9,24,25]. A stably CaSR-transfected HEK293 cell line (HEK293-CaSR clone 1C4) was produced by stably transfecting HEK293 cells with a linearised plasmid containing the full-length cDNA of the human parathyroid CaSR[12]. HEK293-CaSR 1C4 cells were grown in high glucose DMEM (Invitrogen) supplemented with 10% foetal bovine serum and 400 μg/ml neomycin. A high level of CaSR expression in these cells was confirmed by Western blot analysis and immunofluorescence using a mouse monoclonal antibody to human CaSR (ADD; NPS Pharmaceuticals, Salt Lake City, UT, USA)[19,26] . The wild-type and mutant constructs were transiently transfected into HEK-CaSR cells using Lipofectamine 2000 (Invitrogen)[9]. Cells were visualized by a fluorescence microscope (Eclipse E400) with an epifluorescence filter and images captured using a DXM1200C digital camera and NIS Elements software (Nikon)[9,19]. The wild-type and mutants were functionally assessed by measuring the alterations in $[Ca^{2+}]_i$ response to changes in $[Ca^{2+}]_o$, as described[12,19]. Briefly, 48 hours post-transfection, the cells were harvested, washed in calcium- and magnesium-free Hanks' balanced salt solution (HBSS) (Invitrogen) and loaded with 1μg/ml indo-1-acetoxymethylester (Indo-1-AM) (Molecular Probes) for 1 hour at 37°C. After removal of free dye, the cells were resuspended in calcium and magnesium-free HBSS and maintained at 37°C. Flow-assisted cell sorting of transfected cells was performed with a Cytomation MoFlo flow cytometer (Dako-Cytomation, Carpenteria, CA, USA) equipped with an argon laser (Coherent Radiation, Palo Alto, CA, USA), as described[19]. Baseline fluorescence ratio was measured for 2 min, the fluorescence ratio vs time recorded, and data collected for 2 min at each $[Ca^{2+}]_o$. Cytomation summit software was used to determine the peak mean fluorescence ratio of the transient response after each individual stimulus expressed as a normalized response, as previously reported[9,12,19]. Nonlinear regression of concentration-response curves was performed with GraphPad Prism (GraphPad, San Diego, CA) using the normalized response at each calcium concentration for each separate experiment for the determination of the EC_{50} (i.e., $[Ca^{2+}]_o$ required for 50% of the maximal response). Expression of CaSR, AP2σ2 and GFP protein as a surrogate for transfected AP2σ2, was also confirmed by Western blot analysis of cellular protein extract using a rabbit polyclonal antibody to human AP2σ2 (Abcam, Cambridge, UK), a mouse monoclonal antibody to human CaSR (ADD, NPS pharmaceuticals, Salt Lake City, UT), and a monoclonal GFP antibody (Santa Cruz Biotechnology)[19,24].

Enzyme-linked immunosorbent assay (ELISA)

Near confluent stably CaSR-transfected HEK293 cells were transfected with 2μg plasmid DNA per well of 6-well plates as described above, and 24 hours later each well was plated into 24 (3 × 8) wells of a 96 well poly-L-lysine coated plate and incubated overnight. Cells were then starved overnight in 0.5mM Ca^{2+} with 0.2% bovine serum albumin (BSA) in DMEM. Cells were stimulated with either 0.5mM or 5mM Ca^{2+} for 15 minutes at 37°C, placed on ice, briefly washed with ice-cold phosphate buffered saline (PBS), and fixed with either 4% paraformaldehyde (PFA) in PBS (cell-surface CaSR) or methanol (MeOH) (total CaSR) for 15 min, on ice. Subsequent steps were carried out at room temperature. Cells were washed with PBS, blocked for 1 hour in 5% normal goat serum in PBS, and incubated with anti-CaSR antibody (Abcam ab79038) diluted 1 in 200 (PFA-fixed) or 1 in 500 (MeOH-fixed). Cells were washed four times with PBS and incubated with HRP-conjugated goat anti-rabbit antibody (Biorad) diluted 1 in 3000 for 1 hour. Cells were washed four times with PBS and the samples developed with 3, 3′, 5, 5′-tetramethylbenzine (TMB) (Pierce)

for 5 minutes (total CaSR) or 25 min (cell-surface CaSR), the reaction stopped with 2M sulphuric acid, and the absorbances read at 450nm using a Versamax plate reader (Molecular Devices, Sunnyvale, CA). Background (no primary antibody) control was subtracted from each reading and seven replicates for each transfection/fixation were averaged. Data were normalised to cell-surface or total abundance of CaSR in vector-only 0.5mM Ca^{2+} transfected cells.

Analysis of *AP2S1* alternative splicing and expression

Total RNA derived from pooled normal human tissues (Ambion), parathyroid tumours, HEK293 cells or CaSR stably-transfected HEK293 cells were used[24]. First-strand cDNA was produced from 1μg of total RNA using the Quantitect Reverse Transcription Kit (Qiagen)[24]. To investigate alternative splicing, RT-PCR was performed using *AP2S1*-specific primers (Supplementary Table 1) and utilizing 35 cycles with an annealing temperature of 65 °C and with 1.5mM $MgCl_2$[24]. To quantify *AP2S1* expression real-time qRT-PCR was performed with Quantitect gene expression assays (Qiagen) using the Rotorgene-Q system. Ct values were collected for *AP2S1* and the housekeeping genes *GAPDH*, *PGK* and *β2M* during the log phase of the cycle. *AP2S1* levels were normalized to a geometric mean of the three housekeeping genes for each sample and expressed as an arbitrary percentage of the housekeeper geomean expression.

Statistical analysis

The prevalence of *AP2S1* variants was compared to the corresponding prevalence in a large set of control exomes with a Fisher's exact test[32]. For the *in vitro* functional expression studies, the mean EC_{50} from a minimum of twelve separate transfection experiments was used for statistical comparison by using the *F*-test[19].

Supplementary Material

Refer to Web version on PubMed Central for supplementary material.

Acknowledgments

This work was supported by the: United Kingdom Medical Research Council (MRC) programme grants - G9825289 and G1000467 (to M.A.N., F.M.H., A.A.C.R., C.E.T. and R.V.T); National Institute for Health Research (NIHR) Oxford Biomedical Research Centre Programme (to M.A.N. and R.V.T.); High-Throughput Genomics Group, Wellcome Trust Centre for Human Genetics (Wellcome Trust grant reference 090532/Z/09/Z and MRC Hub grant G0900747 91070); Research and Development Office, Northern Ireland (to U.G., S.J.H., and P.J.M.); and Shriners Hospitals for Children (Grant 15958) (to M.P.W.). S.A.H. is a Wellcome Trust Clinical Research training Fellow.

References

1. Collins BM, McCoy AJ, Kent HM, Evans PR, Owen DJ. Molecular architecture and functional model of the endocytic AP2 complex. Cell. 2002; 109:523–535. [PubMed: 12086608]
2. Edeling MA, et al. Molecular switches involving the AP-2 beta2 appendage regulate endocytic cargo selection and clathrin coat assembly. Developmental cell. 2006; 10:329–342. doi:10.1016/j.devcel.2006.01.016. [PubMed: 16516836]
3. Ohno H. Physiological roles of clathrin adaptor AP complexes: lessons from mutant animals. Journal of biochemistry. 2006; 139:943–948. doi:10.1093/jb/mvj120. [PubMed: 16788044]
4. Kelly BT, et al. A structural explanation for the binding of endocytic dileucine motifs by the AP2 complex. Nature. 2008; 456:976–979. doi:10.1038/nature07422. [PubMed: 19140243]
5. McMurtry CT, et al. Significant developmental elevation in serum parathyroid hormone levels in a large kindred with familial benign (hypocalciuric) hypercalcemia. Am J Med. 1992; 93:247–258. [PubMed: 1524075]

6. Lloyd SE, Pannett AA, Dixon PH, Whyte MP, Thakker RV. Localization of familial benign hypercalcemia, Oklahoma variant (FBHOk), to chromosome 19q13. Am J Hum Genet. 1999; 64:189–195. [PubMed: 9915958]
7. Nesbit MA, et al. Identification of a second kindred with familial hypocalciuric hypercalcemia type 3 (FHH3) narrows localization to a <3.5 megabase pair region on chromosome 19q13.3. The Journal of clinical endocrinology and metabolism. 2010; 95:1947–1954. doi:10.1210/jc.2009-2152. [PubMed: 20133464]
8. Pollak MR, et al. Mutations in the human Ca(2+)-sensing receptor gene cause familial hypocalciuric hypercalcemia and neonatal severe hyperparathyroidism. Cell. 1993; 75:1297–1303. [PubMed: 7916660]
9. Hannan FM, et al. Identification of 70 calcium-sensing receptor mutations in hyper- and hypo-calcaemic patients: evidence for clustering of extracellular domain mutations at calcium-binding sites. Human molecular genetics. 2012 doi:10.1093/hmg/dds105.
10. Brown EM, MacLeod RJ. Extracellular calcium sensing and extracellular calcium signaling. Physiological reviews. 2001; 81:239–297. [PubMed: 11152759]
11. Pearce SH, et al. Calcium-sensing receptor mutations in familial benign hypercalcemia and neonatal hyperparathyroidism. J Clin Invest. 1995; 96:2683–2692. [PubMed: 8675635]
12. Pearce SH, et al. Functional characterization of calcium-sensing receptor mutations expressed in human embryonic kidney cells. The Journal of clinical investigation. 1996; 98:1860–1866. doi: 10.1172/JCI118987. [PubMed: 8878438]
13. Kirchhausen T, et al. AP17 and AP19, the mammalian small chains of the clathrin-associated protein complexes show homology to Yap17p, their putative homolog in yeast. J Biol Chem. 1991; 266:11153–11157. [PubMed: 2040623]
14. Heath H 3rd, Jackson CE, Otterud B, Leppert MF. Genetic linkage analysis in familial benign (hypocalciuric) hypercalcemia: evidence for locus heterogeneity. Am J Hum Genet. 1993; 53:193–200. [PubMed: 8317484]
15. Wagener BM, Marjon NA, Revankar CM, Prossnitz ER. Adaptor protein-2 interaction with arrestin regulates GPCR recycling and apoptosis. Traffic. 2009; 10:1286–1300. doi:10.1111/j.1600-0854.2009.00957.x. [PubMed: 19602204]
16. Brown EM, et al. Cloning and characterization of an extracellular Ca(2+)-sensing receptor from bovine parathyroid. Nature. 1993; 366:575–580. doi:10.1038/366575a0. [PubMed: 8255296]
17. Hofer AM, Brown EM. Extracellular calcium sensing and signalling. Nature reviews. Molecular cell biology. 2003; 4:530–538. doi:10.1038/nrm1154.
18. Grant MP, Stepanchick A, Cavanaugh A, Breitwieser GE. Agonist-driven maturation and plasma membrane insertion of calcium-sensing receptors dynamically control signal amplitude. Science signaling. 2011; 4:ra78. doi:10.1126/scisignal.2002208. [PubMed: 22114145]
19. Hough TA, et al. Activating calcium-sensing receptor mutation in the mouse is associated with cataracts and ectopic calcification. Proceedings of the National Academy of Sciences of the United States of America. 2004; 101:13566–13571. doi:10.1073/pnas.0405516101. [PubMed: 15347804]
20. Reyes-Ibarra AP, et al. Calcium-sensing receptor endocytosis links extracellular calcium signaling to parathyroid hormone-related peptide secretion via a Rab11a-dependent and AMSH-sensitive mechanism. Mol Endocrinol. 2007; 21:1394–1407. doi:10.1210/me.2006-0523. [PubMed: 17426287]
21. Leach K, et al. Identification of molecular phenotypes and biased signaling induced by naturally occurring mutations of the human calcium-sensing receptor. Endocrinology. 2012; 153:4304–4316. doi:10.1210/en.2012-1449. [PubMed: 22798347]
22. Guarnieri V, et al. Calcium-sensing receptor (CASR) mutations in hypercalcemic states: studies from a single endocrine clinic over three years. The Journal of clinical endocrinology and metabolism. 2010; 95:1819–1829. doi:10.1210/jc.2008-2430. [PubMed: 20164288]
23. Fang Y, Huang CC, Kain SR, Li X. Use of coexpressed enhanced green fluorescent protein as a marker for identifying transfected cells. Methods in enzymology. 1999; 302:207–212. [PubMed: 12876773]

24. Nesbit MA, et al. Characterization of GATA3 mutations in the hypoparathyroidism, deafness, and renal dysplasia (HDR) syndrome. J Biol Chem. 2004; 279:22624–22634. doi:10.1074/jbc.M401797200. [PubMed: 14985365]
25. Gaynor KU, et al. A missense GATA3 mutation, Thr272Ile, causes the hypoparathyroidism, deafness, and renal dysplasia syndrome. The Journal of clinical endocrinology and metabolism. 2009; 94:3897–3904. doi:10.1210/jc.2009-0717. [PubMed: 19723756]
26. Goldsmith PK, Fan G, Miller JL, Rogers KV, Spiegel AM. Monoclonal antibodies against synthetic peptides corresponding to the extracellular domain of the human Ca2+ receptor: characterization and use in studying concanavalin A inhibition. Journal of bone and mineral research : the official journal of the American Society for Bone and Mineral Research. 1997; 12:1780–1788. doi:10.1359/jbmr.1997.12.11.1780. [PubMed: 9383682]
27. Mounkes L, Kozlov S, Burke B, Stewart CL. The laminopathies: nuclear structure meets disease. Current opinion in genetics & development. 2003; 13:223–230. [PubMed: 12787783]
28. Kim YM, Benovic JL. Differential roles of arrestin-2 interaction with clathrin and adaptor protein 2 in G protein-coupled receptor trafficking. J Biol Chem. 2002; 277:30760–30768. doi:10.1074/jbc.M204528200. [PubMed: 12070169]
29. Nesterov A, Carter RE, Sorkina T, Gill GN, Sorkin A. Inhibition of the receptor-binding function of clathrin adaptor protein AP-2 by dominant-negative mutant mu2 subunit and its effects on endocytosis. The EMBO journal. 1999; 18:2489–2499. doi:10.1093/emboj/18.9.2489. [PubMed: 10228163]
30. Hannan S, et al. Gamma-aminobutyric acid type B (GABA(B)) receptor internalization is regulated by the R2 subunit. J Biol Chem. 2011; 286:24324–24335. doi:10.1074/jbc.M110.220814. [PubMed: 21724853]
31. Clark MJ, et al. Performance comparison of exome DNA sequencing technologies. Nature biotechnology. 2011; 29:908–914. doi:10.1038/nbt.1975.
32. Boyden LM, et al. Mutations in kelch-like 3 and cullin 3 cause hypertension and electrolyte abnormalities. Nature. 2012; 482:98–102. doi:10.1038/nature10814. [PubMed: 22266938]
33. Lunter G, Goodson M. Stampy: a statistical algorithm for sensitive and fast mapping of Illumina sequence reads. Genome research. 2011; 21:936–939. doi:10.1101/gr.111120.110. [PubMed: 20980556]
34. Li H, et al. The Sequence Alignment/Map format and SAMtools. Bioinformatics. 2009; 25:2078–2079. doi:10.1093/bioinformatics/btp352. [PubMed: 19505943]
35. Robinson JT, et al. Integrative genomics viewer. Nature biotechnology. 2011; 29:24–26. doi:10.1038/nbt.1754.
36. Bataille S, Berland Y, Fontes M, Burtey S. High Resolution Melt analysis for mutation screening in PKD1 and PKD2. BMC nephrology. 2011; 12:57. doi:10.1186/1471-2369-12-57. [PubMed: 22008521]
37. Larkin MA, et al. Clustal W and Clustal X version 2.0. Bioinformatics. 2007; 23:2947–2948. doi:10.1093/bioinformatics/btm404. [PubMed: 17846036]

Europe PMC Funders Author Manuscripts

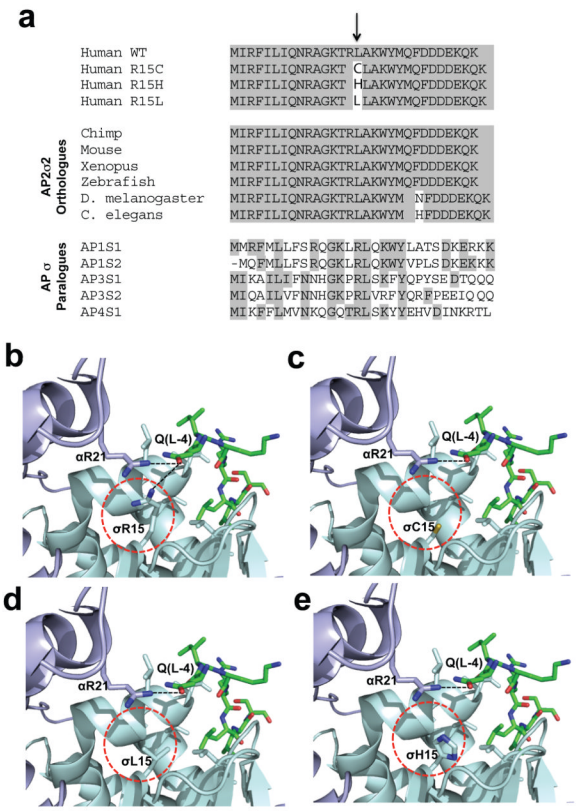

Figure 1. Evolutionary conservation of AP2σ2 Arg15, and structural analysis of mutants

a, Multiple protein sequence alignment of AP2σ2 revealed evolutionary conservation of Arg15 (R15) residues in orthologues and human paralogues. Conserved residues are shaded grey. The Arg15 residue is conserved in all AP2σ2 subunits from human to *C. elegans* and in all human AP sigma subunit paralogues. **b**, Location of Arg15 residue in crystal structure of AP2 heterotetramer bound to an acidic dileucine motif[4]. Polar contacts (black dotted lines) of the Arg15 residue of AP2σ2 (pale-blue) and Arg21 (R21) residue of AP2α1 (mauve) with the glutamine (Q(L-4)) residue of the acidic dileucine peptide (green) are indicated. The AP2σ2 mutants are circled red. The mutants **c**, Cys15 (C15), **d**, Leu15 (L15)and **e**, His15 (H15) are predicted to result in the loss or weakening of this key polar contact.

Europe PMC Funders Author Manuscripts

Europe PMC Funders Author Manuscripts

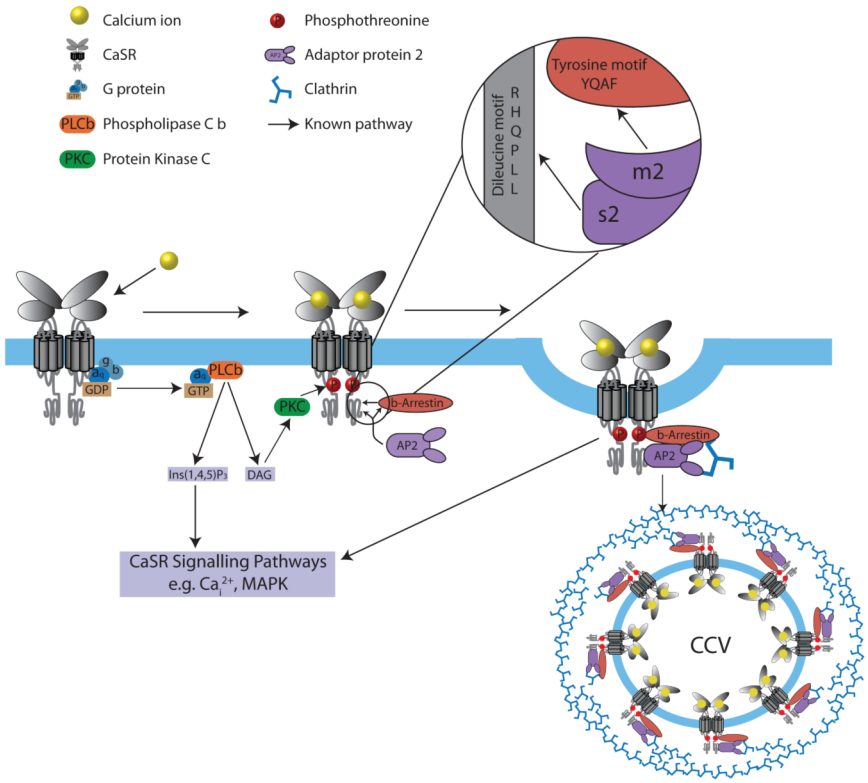

Figure 2. Schematic model for CaSR signaling and its endocytosis mediated by β-arrestin and AP2

Ligand binding of calcium ions (yellow) by the GPCR CaSR (grey) results in G-protein-dependent stimulation, through $G_{q/11}$, of phospholipase C (PLCβ)(orange) activity, causing an accumulation of inositol 1,4,5-trisphosphate (IP_3) and rapid release of calcium ions from intracellular stores (Ca_i^{2+}), as well as an increase in diacylglycerol (DAG) and stimulation of Protein Kinase C (PKC) which phosphorylates CaSR threonine residues (red P) that promotes binding by β-arrestin (brown) and initiates CaSR internalization[10,15,17,28]. AP2 (purple) plays a pivotal role in initiating GPCR internalisation by binding the β-arrestin tyrosine (YxxΦ) motif, via its μ2 subunit; indeed, mutations of the AP2 μ2 subunit disrupt binding to the β-arrestin tyrosine motif and severely impair clathrin-mediated endocytosis[29]. AP2, which is a central component of clathrin-coated vesicles (CCVs), links clathrin to the vesicle membrane and binds to the tyrosine-based and dileucine-based motifs of membrane-associated cargo proteins[1,3]. Internalised GPCR-β-arrestin complexes may signal by G protein-independent pathways e.g. mitogen-activated protein kinase (MAPK) signaling[10,17]. Calcium-stimulation decreases CaSR cell-surface expression[20], and AP2σ2 may facilitate this CaSR internalisation by interaction with a C-terminal dileucine motif (Arg-His-Gln-Pro-Leu-Leu)(RHQPLL)) of the CaSR; indeed studies of the related GPCR, γ-aminobutyric acid type B ($GABA_B$) receptor have shown that removal of this dileucine motif impairs internalisation of this GPCR[30].

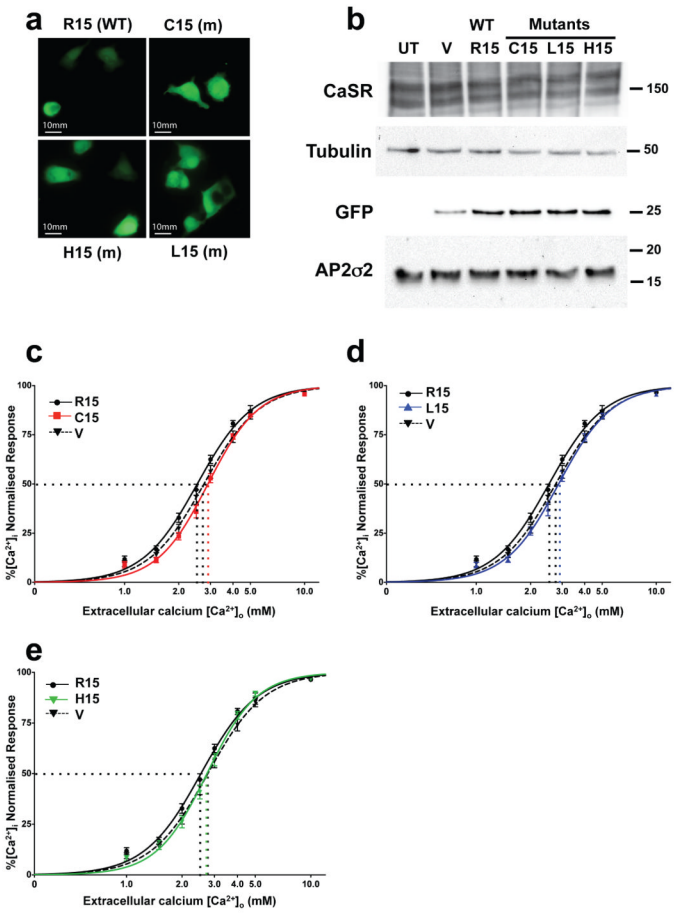

Figure 3. *AP2S1* Arg15 mutants increase EC_{50} of CaSR-expressing cells

HEK293 cells stably transfected with CaSR were transiently transfected with wild-type (WT) or mutant (m) *AP2S1*-pBI-CMV2-GFP expression vector, or the empty vector pBI-CMV2-GFP. **a**, Fluorescence microscopy confirmed GFP expression and successful transfection[19,24]. **b**, Western blot analysis, using anti-CaSR, anti-tubulin, anti-GFP, and anti-AP2σ2 antibodies[19,24-26]. HEK293 cells endogenously express AP2σ2 (Supplementary Fig. 2), and co-expression of mutant AP2σ2 mimicked the situation occurring in FHH3 patients (Supplementary Fig. 1). Transfection with WT or m *AP2S1*-pBI-CMV2-GFP vector resulted in a significantly greater expression of AP2σ2 by 1.5 to 2.3-fold ($p<0.05$) when normalised for tubulin expression and compared to transfection with empty vector (data not shown). UT-untransfected cells and V-empty vector. **c**-**e**, $[Ca^{2+}]_i$ responses (mean±SEM, n=12) to changes in $[Ca^{2+}]_o$ of cells transfected with *AP2S1* WT, mutant (m) or vector (V) alone; the vector expressed GFP but not AP2σ2, whereas the WT and mutant constructs expressed GFP and either WT or mutant AP2σ2, respectively. **c**, Cys15 (C15), **d**, Leu15 (L15), and **e**, His15 (H15) constructs. EC_{50} values (dotted lines).

Europe PMC Funders Author Manuscripts

Table 1

Biochemical features of 13 FHH families or patients

Mutation (base change)	Family/ Patient	Sex of affected members	Age at diagnosis (years)	Serum				Urine
				Calcium (mmol/l)[a]	Phosphate (mmol/l)[b]	Alkaline phosphatase (U/L)[c-f]	PTH[g-i]	Calcium[j-l]
Arg15Cys (CGC→TTGC)								
	FHH_{Ok}[m]	13F, 3M[o]	36 ± 6.6[p]	2.88 ± 0.03	0.77 ± 0.03	73 ± 10[c]	65 ± 17.0[g]	0.003 ± 0.001[j]
	FHH^{Nl}_{m}	11F, 5M	32 ± 4.4	2.72 ± 0.07	0.95 ± 0.03	99 ± 18[d]	60 ± 6.2[h]	0.006[n]
	02/08[n]	2F	19	2.77	0.83	243[e]	3.3[i]	0.006[j]
	02/10	M	78	2.74	0.84	220[e]	45.1[h]	0.18[k]
	03/96	M	<15	H	N	N	N	L
	07/98[n]	2F	16	H	N	N	N	L
Arg15Leu (CGC→CTC)								
	13/07	F	51	3.03	0.71	57[d]	6.2[i]	1.6[l]
	11/02[n]	2M, 1F	52	3.19	1.11	63[d]	49[h]	0.35[k]
	04/10	M	11	3.13	0.91	316[f]	45[h]	0.32[k]
	19/07[n]	1M, 2F	0.02	3.3	N	165[f]	54[h]	0.1[k]
Arg15His (CGC→CAC)								
	04/04	F	19	2.85	N	N	36[h]	0.025[j]
	23/08	M	73	2.62	0.83	164[e]	49.6[h]	0.23[k]
	11/10	F	49	2.72	0.97	133[e]	11.2[i]	0.8[l]

Normal serum ranges[11]:

[a] calcium, 2.10-2.60 mmol/l;

[b] phosphate, 0.70-1.40 mmol/l; alkaline phosphatase activity,

[c] 22-84 U/l,

[d] 35-120 U/l,

[e] 70-330 U/l,

[f] 60-400 U/l; PTH,

[g] 12-34 pg/ml,

[h] 10-70 pg/ml,

[i] 1.3-7.6 pmol/l; Normal urine ranges[11]:

[j] calcium:creatinine clearance ratio >0.01;

[k] random calcium:creatinine ratio >0.7;

[l] 24-hour calcium excretion >4 mmol/24-hours;

[m] Details of families from previously published reports[5-7];

[n] Known family history and details from probands only provided;

[o] M, male, F, female;

[p] Values are shown as mean ± SEM; Exact value not available but reported to be H, high; N, normal; L, low.

Europe PMC Funders Author Manuscripts

Europe PMC Funders Author Manuscripts

Table 2

EC_{50} values of AP2S1 wild-type and FHH3-associated mutants.

AP2σ2	EC_{50} (mM)	95% CI (mM)	p v WT	p v V
Vector (V)	2.76	2.69-2.84	**	-
Arg15 (WT)	2.53	2.47-2.59	-	**
Cys15 (m)	2.90	2.85-2.96	**	*
Leu15 (m)	2.86	2.80-2.93	**	ns
His15 (m)	2.73	2.66-2.80	**	ns

Table 3

Effects of FHH3-associated *AP2S1* mutation (Arg15Cys) on CaSR cell-surface expression.

	Total CaSR		Cell-surface CaSR	
	0.5mM Ca^{2+}	**5mM Ca^{2+}**	**0.5mM Ca^{2+}**	**5mM Ca^{2+}**
Vector	100±1.4	101.9±2.3	100±4.9	47.1±3.6[a*]
WT (Arg15)	99.3±2.8	104.6±0.9	93±4.2	28.1±2.0[b*,d*,e#]
Mutant (Cys15)	92.6±1.3	98.6±2.3	98.1±2.8	47.1±6.3[c*]

HEK293 cells which stably expressed the CaSR were transfected with WT (Arg15) *AP2S1,* mutant (Cys15) *AP2S1* or vector-only constructs, treated with either 0.5mM Ca^{2+}_o or 5.0mM Ca^{2+}_o for 15 minutes, and cell-surface and total expression of CaSR measured using an intact cell ELISA[18]. Results were normalised to vector-only transfected cells, as previously reported[18], and shown as mean±SEM (n=6) for each experiment. Comparison of total CaSR at 0.5mM and 5mM revealed no significant difference. Comparison of cell-surface CaSR expression revealed significant differences as follows:

[a] Compared to Vector (0.5mM);

[b] Compared to WT (0.5mM);

[c] Compared to Mutant (0.5mM);

[d] Compared to Vector (5mM);

[e] Compared to Mutant (5mM).

* $p<0.005$,

# $p<0.05$.